TECHNICAL MEMORANDUM

700

Characterising channel center frequencies in AMSU-A and MSU microwave sounding instruments

Qifeng Lu[1] and William Bell[2]

Research Department

[1] National Satellite Meteorological Center, China Meteorological Administration, Beijing, China

[2] Met Office, Exeter, UK

Submitted to *Journal of Atmospheric and Oceanic Technology*

May 2013

European Centre for Medium-Range Weather Forecasts
Europäisches Zentrum für mittelfristige Wettervorhersage
Centre européen pour les prévisions météorologiques à moyen

Series: ECMWF Technical Memoranda

A full list of ECMWF Publications can be found on our web site under:
http://www.ecmwf.int/publications/

Contact: library@ecmwf.int

European Centre for Medium-Range Weather Forecasts
Shinfield Park, Reading, RG2 9AX, England

Abstract

Passive microwave observations from the Microwave Sounding Unit (MSU) and the Advanced Microwave Sounding Unit-A (AMSU-A) have been exploited widely for numerical weather prediction (NWP), atmospheric reanalyses and for climate monitoring studies. The treatment of biases in these observations, both with respect to models as well as between satellites, has been the focus of much effort in recent years. In this study we present evidence that shifts, drifts and uncertainties in pass band center frequencies are a significant contribution to these biases. Center frequencies for AMSU-A channels 6-14 and MSU channel 3 have been analysed using NWP fields and radiative transfer models, for a series of operational satellites covering the period 1979 - 2012. AMSU-A channels 6 (54.40 GHz), 7 (54.94 GHz) and 8 (55.50 GHz) on several satellites exhibit significant shifts and drifts relative to nominal pass band center frequencies. No significant shifts were found for AMSU-A channels 9-14, most probably as a consequence of the active frequency locking of these channels. For MSU channel 3 (54.96 GHz) most satellites exhibit large shifts, the largest for the earliest satellites. For example for the first MSU on the TIROS-N satellite the analysed shift is 68 MHz over the lifetime of the satellite. Taking account of these shifts in the radiative transfer modelling significantly improved the fit between model and observations, eliminates the strong seasonal cycle in the model-observation misfit and significantly improves the bias between NWP models and observations. The study suggests that, for several channels studied, the dominant component of the model-observation bias results from these spectral errors, rather than radiometric bias due to calibration errors.

1 Introduction

In the last three decades microwave radiance observations from polar orbiting satellites have been exploited widely for operational numerical weather prediction (NWP) and for climate studies assessing long term trends in atmospheric temperatures. Observations from discrete channels in the 50-58 GHz range of the microwave spectrum have been particularly valuable in providing altitude resolved information on atmospheric temperature, albeit at relatively coarse vertical resolution. It has long been known that this type of observation suffers from biases, of several tenths of a Kelvin in measured brightness temperatures, relative to NWP model fields as well as between nominally identical observations from instruments on different satellites. This paper shows that, for many key tropospheric and lower stratospheric temperature sounding channels on past and present operational satellites, a significant component of these biases results from shifts, drifts and uncertainties in the central frequencies of channels. The magnitude of these uncertainties, at several tens of MHz, is larger than previously thought.

The continuity provided by an operational series of satellite instruments is critical for both weather and climate applications of microwave data. The first such instrument, the Microwave Sounding Unit (MSU) (Mo et al. (2001)) was launched on the Television Infrared Observation Satellite-N (TIROS-N) satellite in 1978. A further eight MSU instruments were successfully launched, the last in the series on the National Oceanographic and Atmospheric Administration's NOAA-14 satellite in 1994. The four channel MSU instruments were succeeded by the fifteen channel Advanced Microwave Sounding Unit-A (AMSU-A) instruments in 1998 (Goodrum et al. (2000)). These instruments continue to operate on seven operational satellites at the present time. This long series of microwave measurements is expected to continue for the next two decades at least. In the immediate future (5-10 years), continuity will be provided by launches planned by satellite agencies in the US, Europe and China. At the present time, there is an expectation that within five years the international scientific community will have collected a continuous record of passive microwave observations in the 57 GHz O_2 absorption band spanning forty years. This provides a strong incentive to develop a detailed understanding of biases caused by instrumental effects, as well as deficiencies in radiative transfer modelling.

The observations from the AMSU instruments are assimilated directly as radiances using variational assimilation schemes (e.g. Courtier et al. (1994), Rawlins et al. (2007)). In current NWP systems microwave observations, taken collectively as a system, provide the greatest contribution to forecast accuracy (Cardinali (2009)) amongst the range of observation types currently assimilated.

Significant biases exist between microwave observations and simulated observations based on short range NWP forecast fields. A requirement of data assimilation systems is that observations are unbiased relative to the assimilating model. It has, therefore, been necessary to develop schemes for bias correcting the observational data prior to assimilation. For the early MSU sensors, global mean biases, relative to current NWP models, are in the range $\pm$1.0K in measured brightness temperatures (for example for MSU channel 2, Dee and Uppala (2009)). For AMSU-A observations these biases are typically smaller, for example for channels 6 and 7 they fall in the range $\pm$ 0.65K during the period 1998–2008 (Dee and Uppala (2009)). These global bias values obscure more complex geographical variation.

During the development of early bias correction schemes (Harris and Kelly (2001) and references therein) it was noted that the bias fields showed a strong correlation with air mass (thickness between two levels in the atmosphere obtained through integration of the hydrostatic equation). Possible causes of the biases were identified as unresolved errors in the radiative transfer modelling (termed here spectral errors) as well as radiometric calibration errors (termed here radiometric errors)(McNally et al. (2000)). Spectral errors could result from uncertainties in the underlying spectroscopy, for example in the linestrengths or linewidths of O_2 absorption lines, or through uncertainties in instrument parameters, for example errors in the pass band center frequencies or band shape. Radiometric errors, as defined here, encompass a group of errors related to the calibration of the instrument on-orbit and include radiometric offsets, inaccuracies in antenna pattern corrections, errors in target temperature and emissivity, as well as errors related to radiometer non-linearities. Linear models were developed to predict the magnitude of the biases, from model variables at the location of the observation. These models were very effective in significantly reducing the magnitude of global mean biases as well as the variance of model-observation differences and such schemes remain a key component of NWP data assimilation systems. The coefficients of these schemes can be determined offline in static bias correction schemes and are updated from time to time if global biases change significantly. More recently variational bias correction schemes have been developed (Auligné et al. (2007)) in which the coefficients of the correction are determined variationally as part of the assimilation process and are actively updated in each assimilation cycle. In both of these approaches the corrections are based on empirical error models and they make no attempt to partition the bias into underlying physical mechanisms. Variational bias corrections form an essential component of modern reanalysis systems (Dee and Uppala (2009)), in which the automated and continuous tuning of the biases replaces the impractical *ad-hoc* tuning required of a static scheme. In addition to deal with radiative transfer modelling errors more accurately a scheme has been used at ECMWF in which the optical depths in each atmospheric layer are scaled by a constant value, γ, (Smith et al. (1983)) determined by minimising first guess departure variances with respect to γ.

There are several potential limitations of the current schemes. Firstly the error model, although explaining much of the variance in the innovation distribution, is based on a strong correlation between the predictors and the observed biases but is not based on an accurate representation of the underlying processes causing the biases and therefore may fail to model local biases completely. Secondly the application of bias corrections, based on an incomplete representation of the underlying mechanisms, could be perceived as a weakness when the data is used to analyse trends in atmospheric temperatures from reanalysis products for climate applications.

The continuity provided by the MSU/AMSU-A series, coupled with their relative insensitivity to the radiative effects of clouds for many key channels, has led to them being used by several groups for

the analysis of decadal temperature trends, initiated by the study of Christy et al. (1998). Since this work much effort has been devoted to understanding and minimising intersatellite biases as a first step in the construction of climate datasets. Increasingly sophisticated analyses (Mears and Wentz (2009), Zou and Wang (2011)) have uncovered a number of effects which cause these biases, including, radiometer non-linearities, channel frequency offsets (Iacovazzi et al. (2009)) , calibration errors and solar heating induced thermal effects. Uncertainties remain, however, concerning the underlying physical mechanisms for the observed biases for many channels. This uncertainty contributes to the form and magnitude of residual biases for any given correction scheme and therefore contributes to uncertainties in climate trends derived from the data.

In a recent investigation into the on-orbit performance of China's FY-3A (Dong et al. (2009)) Microwave Temperature Sounder (MWTS) Lu et al. (2011a) discovered that large brightness temperature biases relative to the ECMWF model were the result of uncertainties in channel center frequencies. A method was developed to derive improved estimates of the channel center frequencies and the resulting corrected data had lower biases relative to the ECMWF model, was similar in quality to equivalent channels from AMSU-A, and gave improved analyses and forecasts when introduced into the ECMWF system (Lu et al. (2011b)).

In this study we extended this analysis to the series of MSU and AMSU-A instruments dating back to 1979. The analysis is restricted to AMSU-A channels 6-14. Channels 1-5 are not included due the difficulty in screening observations reliably for cloud effects. This is not anticipated to be a fundamental limitation of the technique and this analysis will be a topic for further study. For MSU, only channel 3 is considered due to similar difficulties with channels 1 and 2. Another possible cause of radiative transfer biases, which could be manifested as an air mass dependent bias, is errors in the underlying spectroscopy. In this study we assess the effect of newly available spectroscopic parameters for the 50-60 GHz O_2 absorption complex (Tretyakov et al. (2005)) on the pass band shift analysis reported here.

In Section 2 we describe briefly the method used to derive the improved channel center frequency estimates. In Section 3 we present the results for the operational AMSU-A sensors for the period 1998 - 2012. In Section 4 we present an analysis of the analysed pass band centers during the period 1978-2007 for MSU channel 3. In Section 5 we conclude with some discussion on the results.

2 Method

The principle of the method to derive improved estimates of the channel center frequencies, expressed here as a shift ($\Delta\nu$) of the true pass band center frequency (ν) relative to the nominal pass band center (ν_0), is based on the link between $\Delta\nu$ and the complex state-dependent biases between observations and simulations based on NWP model fields. In brief, the variance of the (observed - simulated) brightness temperature differences for an ensemble of observations is minimised by varying the assumed pass band center frequency for each channel considered. The method relies on the high accuracy of short range forecast fields from NWP models as well as that of a radiative transfer model used to map atmospheric states to simulated brightness temperatures.

To expand on this brief description: any errors in the assumed channel center frequencies will result in a microwave channel sampling optically deeper, or shallower, parts of the O_2 absorption spectrum. This results in a vertical displacement of the channel weighting function which, depending on the temperature lapse rate at the observation location, will in turn result in a bias in measured brightness temperatures (relative to those obtained from an unshifted pass band). These errors are manifested as an airmass dependence of the biases between model and observations. Previous studies (Peubey et al. (2011)) have

shown that these errors can also result in a cross-scan dependence of the bias.

Such errors in the assumed center frequency may arise from errors in the pre-launch measurement, or real shifts or drifts in the local oscillator frequency on-orbit. It will be demonstrated in this paper that errors arising from both shifts and drifts on-orbit are evident in the MSU and AMSU-A instruments.

The approach here follows that described by Lu et al. (2011a) for the analysis of pass band errors in the FY-3A MWTS instrument, so only the main elements are described here. The method uses a line-by-line radiative transfer model to simulate observations using short range forecast fields from the ECMWF NWP model. For the long time series analysis of pass band drifts in AMSU-A (Section 3) and MSU (Section 4) model analysis fields from the ERA-Interim atmospheric reanalysis (Dee et al. (2011)) were used. The model fields are interpolated to the location of the observations. The simulated brightness temperatures can then be compared with observations, typically for an ensemble of 5-15,000 observations over a 12 hour period, giving full global coverage from the ensemble. These differences are routinely calculated in NWP data assimilation systems and are commonly referred to as innovations, or first guess departures. The standard deviation of the first guess departures can then be used as a measure of the misfit between observations and simulations. The process is repeated for incremental shifts of the assumed center frequencies over a range of $\pm$ 100 MHz from the nominal pass band center frequency, in steps of 1 MHz. The center frequency associated with a minimum in the standard deviation of the first guess departures yields the new estimate of the pass band center frequency. Additionally, to attribute significance to the derived shifts, we impose the condition that any estimated shift in the pass band center frequency from the nominal value should be accompanied by a significant improvement (of 10 % or more) in the fit between simulations and observations, *ie* a non-zero frequency shift should account for a significant fraction of the variance in the uncorrected first guess departures. The threshold of 10% is discussed in more detail in Section 3.3.4.

Figure 1 shows the example of NOAA-16 channel 6 for an ensemble of observations. A shift of +30 MHz from the nominal pass band center frequency of 54.40 GHz results in a significant reduction in the standard deviation of the departures (17%). As a consequence of the +30 MHz shift the magnitude of the mean departure is also significantly reduced, from a value of -0.8K assuming the nominal center frequency to -0.1K at the new center frequency.

Figure 2(a) shows a map of differences between observed and simulated brightness temperatures from ECMWF first guess model fields, for NOAA-16 AMSU-A channel 6, for the 12 hour assimilation cycle centred at 12Z on 23 August 2011, assuming the nominal pass band centre frequency of 54.40 GHz. Using instead the estimated centre frequency of 54.43 GHz, Figure 2(b) shows that accounting for the shifted pass band brings the field of observed minus simulated brightness temperatures closer to zero. Also, much of the strong latitudinal variation in the departures is reduced. The dominant feature remaining is the strong asymmetric cross-scan bias. It results from spacecraft intrusions into the instrument field of view. After application of the variational bias correction, the departure fields in Figures 2 (c) and (d) look fairly similar. This indicates that variational bias correction is effective in eliminating most of the structure resulting from the bias induced by the frequency shift. It is noteable that the correction of the cross-scan bias appears marginally better for the new pass band simulations. Previous studies (Peubey et al. (2011)) have shown that errors due to pass band shifts are manifested as airmass dependent and cross-scan biases. In the present case, it appears that the pass band shift correction is reducing the amplitude of the cross-scan bias. As a result, this residual cross-scan bias can be corrected more effectively by the variational bias correction scheme. Note, in the operational use of the data at ECMWF, which assumes a nominal frequency for all AMSU-A instruments, the outermost three spots in the AMSU-A swath are blacklisted to avoid using data affected by the large residual cross-scan biases.

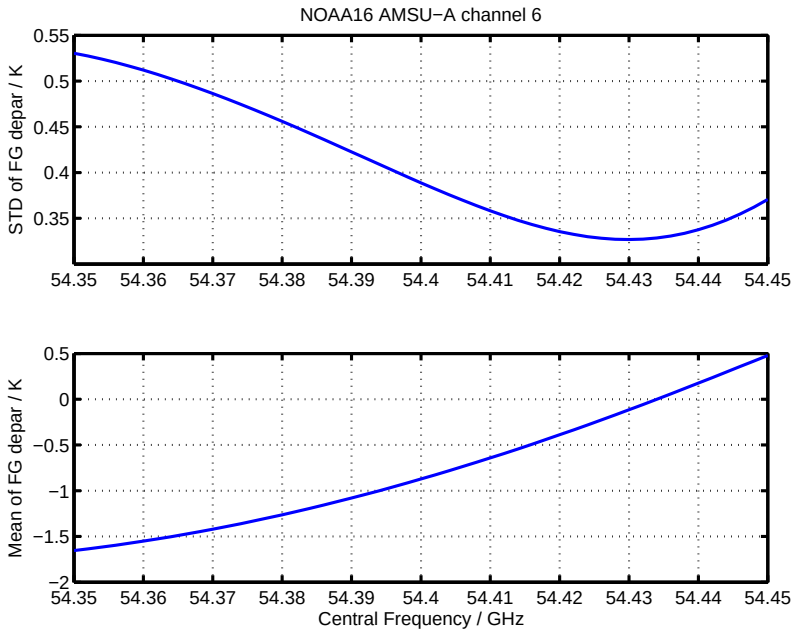

Figure 1: The effect of shifting the channel center frequency for NOAA-16 channel 6, with a nominal center frequency 54.40 GHz. The top panel shows the effect on the standard deviation of first guess departures. The bottom panel shows the effect on the mean first guess departures.

As stated earlier, an assumption in this approach is that the model fields serve as a reasonable proxy for the true atmospheric state and differences between observations and simulations are reasonably interpreted as errors from which, in this particular study, frequency shifts are being analysed. Based on recent experience in characterising biases in microwave sounder data from SSM/I-S (Bell et al. (2008)) and MWTS (Lu et al. (2011a)) this appears to be a valid assumption. Errors in the model background fields, mapped to observation space, are estimated to be in the range 50-100 mK for the tropospheric and lower stratospheric sounding channels of AMSU-A. The high accuracy of the model short range forecast fields results from the large number of observations used to determine the initial conditions (the analysis). Of particular importance, with respect to the accuracy of the temperature fields in the mid-troposphere to lower stratosphere, are multivariate (temperature, humidity, wind) observations from radiosondes, satellite observations from the advanced infrared sounders (AIRS and IASI, see Collard and McNally (2009)) and data from a constellation of global positioning system radio occultation (GPSRO) satellite instruments (Healy and Thépaut (2006)). The GPSRO observations, assimilated as bending angles, have small absolute uncertainties in the mid-troposphere to lower stratopshere and are assimilated without bias correction, thereby anchoring the NWP system.

The effects of pass band shifts are expected to result in biases similar in geographical form to those resulting from errors in spectroscopic parameters. Specifically, significant errors in line strengths or pressure broadening coefficients are expected to produce similar bias patterns. The line-by-line model used in this study is the Millimetre Wave Propagation model of Liebe et al. (1992) (hereafter, MPM92). New coefficients for this model have recently become available (Tretyakov et al. (2005)), based on new measurements of the O_2 absorption complex at a range of low (to 5.3 hPa) pressures as well as atmospheric pressures. Tretyakov et al. (2005) include updates to the coefficients of the MPM92 model, for example line intensities are modified by up to 2%. The new coefficients were used, in addition to those

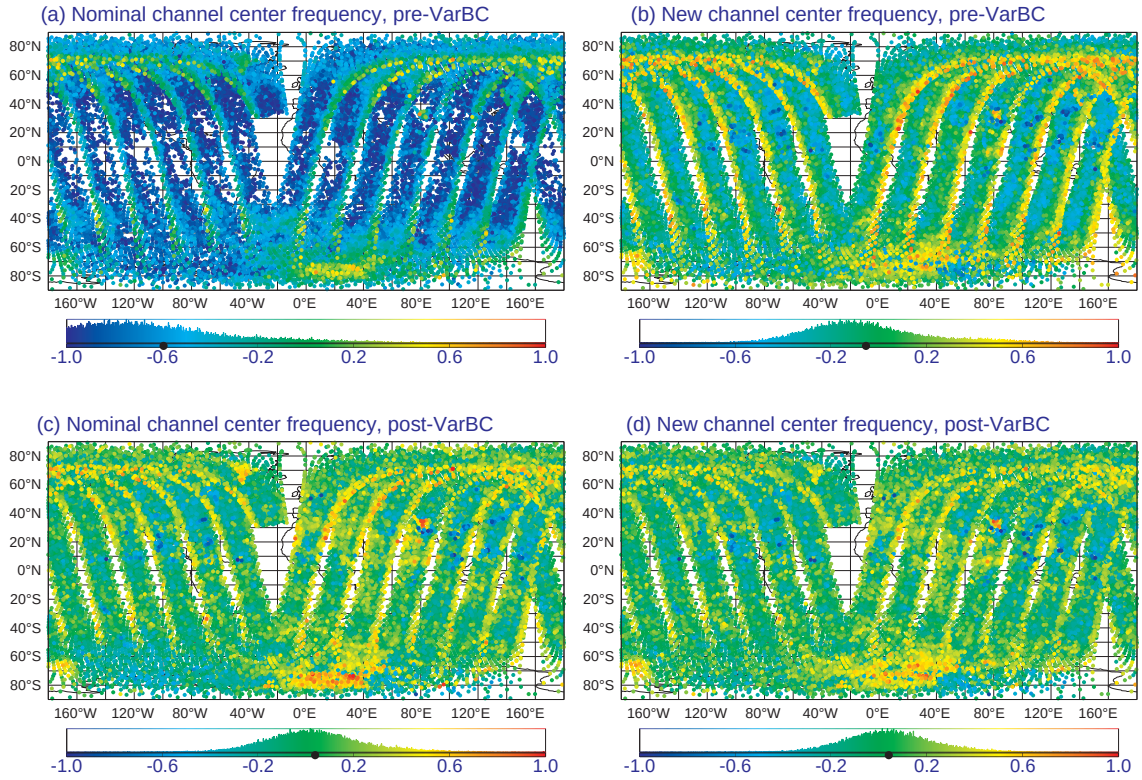

Figure 2: Effect of the optimised center frequency estimates for NOAA-16 channel 6 (54.40 GHz) on first guess departure fields for the 12 hour assimilation cycle centered at 12Z on 23 August 2011, both before ((a) and (b)) and after ((c) and (d)) variational bias correction.

of MPM92, in order to assess the sensitivity of the pass band shift results to uncertainties in these key spectroscopic parameters.

3 Frequency drift analysis for AMSU-A sensors

3.1 Frequency Shifts and the Effect of New O_2 Spectroscopy

Figure 3 shows the analysed frequency shifts for AMSU-A instruments from satellites NOAA-15, NOAA-16, NOAA-18, NOAA-19, MetOp-A and NASA's EOS-Aqua for channels 6-14. The analysed shifts using the new spectroscopy of Tretyakov et al. (2005) are also shown in Figure 3. This analysis is based on an ensemble of 15 000 observations from a single 12-hour assimilation cycle centered on 00Z on 18 August 2011. Figure 4 shows the reduction in first guess departure standard deviations when these shifted pass bands are assumed relative to nominal values. The optimised estimates of the center frequencies are shown in Table 3.

Several features are striking in Figure 3. Firstly the analysed shifts are large for several channels on most instruments. The largest shifts, at several 10s MHz, are found for the tropospheric temperature sounding channels 6, 7 and 8. Correcting these large shifts, in most cases, results in large reductions in the variance of the first guess departures. The pass band stability specifications for channels 6, 7 and 8 of the AMSU-A instrument are ± 5, ± 5 and ± 10 MHz (JPL (2000)) so it appears that several channels are out of specification. Secondly, there appears to be a clear division between the shifts diagnosed for channels 6-8 and channels 9-14. For channels 6-8 the large analysed shifts are associated with significant reductions in the standard deviations of the first guess departures. In contrast the analysed shifts for channel 9-14 are usually smaller and are associated with much smaller reductions in the variance of the first guess departures.

A possible explanation for this is that channels 9-14 are served by a single local oscillator (LO) operating at 57.29 GHz (JPL (2000)) which is stabilised in frequency by means of a reference (143.2 MHz) crystal oscillator and a phase locked loop (PLL). This active locking of the local oscillator is necessary for the very narrow pass bands of channels 12-14 (bandwidths ranging from 3 – 16 MHz) where even small drifts could result in significant measurement error. For channels 6-8, with bandwidths in the range 330–400 MHz the LO is free-running and the assumption to date has been that the passive thermal stability of the oscillator, coupled with small temperature tuning coefficients, ensures the shifts are acceptably small (Peubey et al. (2011)).

It is possible that other errors in the radiative transfer modelling, for example in the spectroscopic parameters or in the assumed satellite view geometry, could be manifested in a very similar bias signal as pass band shift and hence these other errors could be aliased into the shift estimate. An indication of a spectroscopic error would be a consistent signal across all sensors and, most likely, a coherent channel dependence. The inter-satellite differences in the derived shifts make it unlikely that the shifts are due solely to a spectroscopic error. Although the possibility remains that some component of the analysed shifts is due to spectroscopic errors the simplest explanation of these results is that the spectroscopic errors have a small impact on the derived center frequencies, the shifts analysed for channels 6-8 are accurate, and that the phase locking of the 57.29 GHz LO is very effective in stabilising the center frequencies for channels 9-14.

Regarding the impact of the new O_2 spectroscopy, the results for channels 6-8 are not changed significantly. The largest analysed shifts for channels 9-14 are observed for channels 9 and 10 with shifts of

up to 30 and 18 MHz for the MPM92 spectroscopy. However only the shift for channel 10 is associated with near-significant reductions in the first guess departure standard deviation (7.2 %). Furthermore the analysed shifts for channel 10 are reduced from 12.3 to 8.7 MHz, averaged over all sensors, using the new spectroscopy.

3.2 NWP model dependence of the shifts

Despite the recent successful approach of using NWP forecast fields and radiative transfer modelling to diagnose instrument problems there remains a reasonable concern that errors in NWP models are aliased into apparent pass band shifts. For example, model errors which show a strong latitudinal dependence could, conceivably, result in an erroneous analysed shift.

As a test of this hypothesis the analysis was repeated using fields from global models from additional NWP centers: the National Center for Environmental Prediction (NCEP, US); the Met Office (UK) and China's Meteorological Administration (CMA). The main features of these models are summarised in Table 2. The shifts derived in this analysis are shown in Figure 5, the reduction of the standard deviation of the departures in Figure 6 and the values given in Table 4. The analysis was based on the same assimilation cycle for all models (00Z on 18 August 2011). The analysis is restricted to channels 6-11 as the relatively low model tops for the NCEP and CMA models (0.1 hPa) prevents a meaningful analysis for channels 12, 13 and 14. The results from the NCEP, UKMO and CMA models are in broad agreement with the ECMWF results: the derived shifts are large for channels 6-8 and smaller for channels 9-11. These results further support the conclusion that the derived shifts are not a consequence of model biases, but most likely reflect real uncertainties in the central frequencies for channel 6, 7 and 8.

3.3 Time series of AMSU-A pass band center frequencies for channels 6 to 8.

The analysis was extended to cover the entire AMSU-A data record, from 1998–2012, in order to assess the long term behaviour of the shifts. In this investigation analysis fields from the ECMWF ERA-Interim Reanalysis (Dee et al. (2011)) were used and the analysis was repeated on the 15th day of each month. The main features of the ERA-Interim reanalysis are summarised in Table 2.

The results of this analysis are summarised in Figures 7 to 12 for channels 6 to 8, respectively, for NOAA-15 to -19, as well as MetOp-A, and EOS-Aqua. For each channel, the results are presented in two figures for clarity. Time series for NOAA-15, -16 and -17 are shown in Figures 7, 9, and 11 and time series for NOAA-18, -19, MetOp-A, and EOS-Aqua are shown in Figures 8, 10, and 12 We first describe the general features found in Figures 7–12.

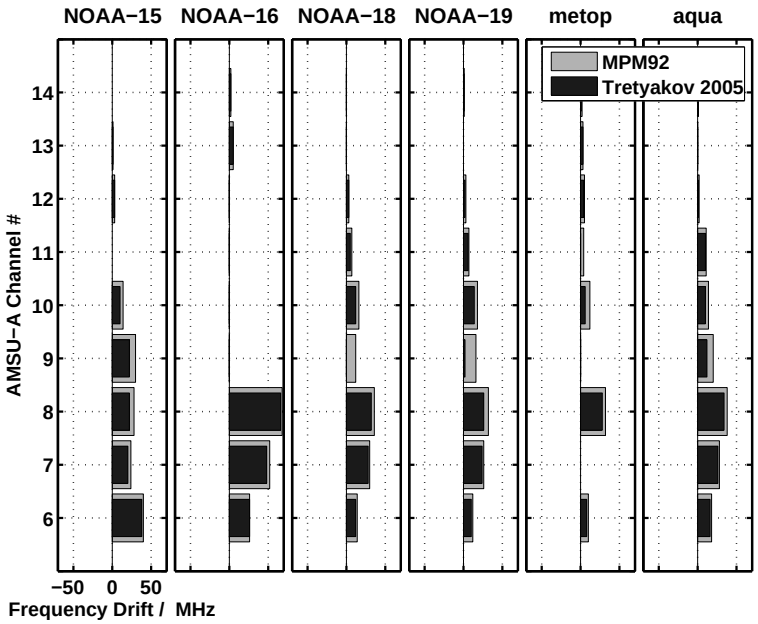

Figure 3: The derived pass band shifts for AMSU-A channels 6-14 for NOAA, MetOp and NASA Aqua satellites, obtained from an analysis of departures from 00Z on 18 August 2011. Results are shown for MPM92 spectroscopy (Liebe et al. (1992)) (grey bars) and for new spectroscopic parameters from Tretyakov et al. (2005) (black bars).

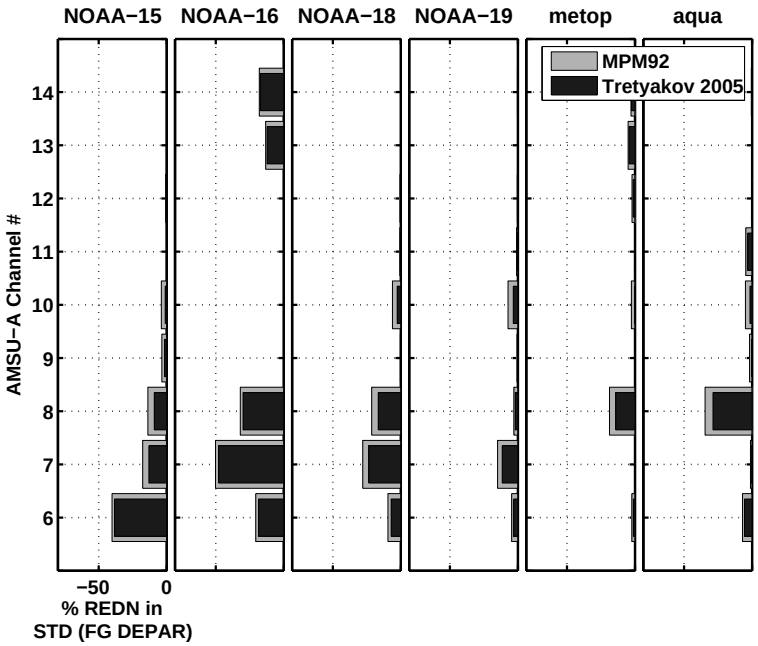

Figure 4: Reductions in the standard deviations of first guess departures achieved using the optimised estimates of the channel center frequencies shown in Figure 3 for the cycle centered at 00Z on 18 August 2011.

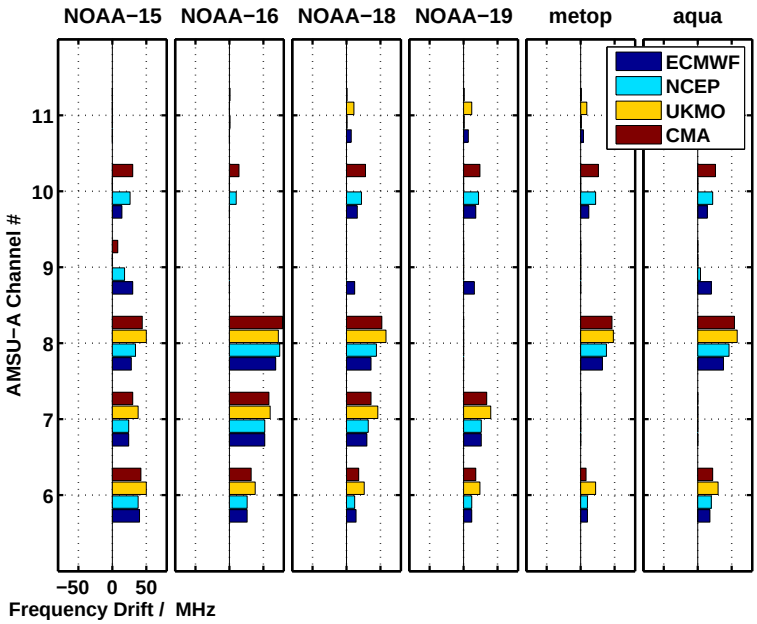

Figure 5: Shifts in channel center frequencies derived using fields from four different NWP models: The European Centre for Medium Range Weather Forecasting (ECMWF); National Center for Environmental Prediction (NCEP); Met Office (UKMO) and China's Meterorological Administration (CMA). The analysis was performed using approximately 15 000 observations from the 12 hour assimilation cycle centered on 00Z on 18 August 2011.

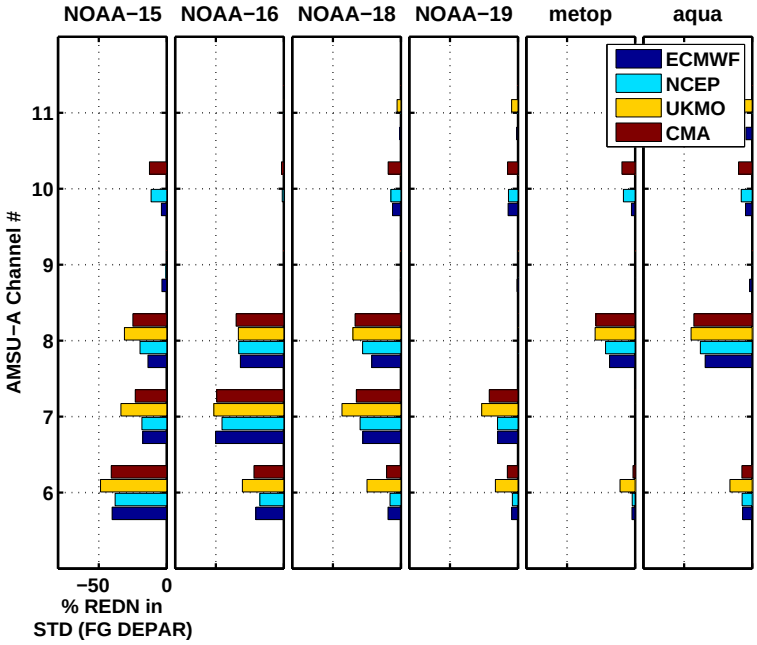

Figure 6: Reductions in the standard deviations of first guess departures achieved using the optimised estimates of the channel center frequencies shown in Figure 5.

For channel 6, the frequency shifts in the top panels of Figures 7 and 8 are generally large, at around 10–20 MHz for the early post-launch phase for the earlier instruments (NOAA-15, -16, -17 and EOS-Aqua). The more recent instruments (NOAA-18, -19, and MetOp-A) exhibit smaller shifts, around 10 MHz. This may reflect improved pre-launch measurement accuracy, or more stable local oscillators in the more recently launched instruments. For NOAA-15 channel 6 we observe a large temporal drift, from about 20 MHz in 1998 to more than 40 MHz in 2012. This is discussed in more detail below. For channels 7 and 8, there appears to be a stable shift of 24–38 MHz for all functioning sensors, except for NOAA-16, whose case is discussed in more detail below.

The middle panels of Figures 7–12 show the standard deviations of the first guess departures computed with the new pass band estimates (circles), compared with those computed with the nominal pass band specifications (triangles). For channels and satellites which show a strong seasonal cycle in the standard deviation of first guess departures, the seasonality is virtually eliminated in most cases by using estimated pass band centre frequencies instead of nominal pass band centre frequencies.

The lower panels of Figures 7–12 show the mean of the first guess departures computed with the new pass band estimates (circles), compared with those computed with the nominal pass band specifications (triangles). For almost all channels the mean departures are significantly closer to zero when the estimated pass band frequencies are used instead of the nominal pass band frequencies. In most cases, the residual bias is smaller than 0.5K. This is a significant finding which suggests that the radiometric calibration of the instruments is probably better than would first appear from the biases computed from nominal pass band frequencies. An exception here is MetOp-A channel 8, for which the mean departure is significantly larger after correction for the channel shift, despite a clear improvement in the variance and seasonality of the departures. The discontinuity for MetOp-A channel 8 is due to a change in the antenna pattern correction during May 2007, also evident for channels 6 and 7.

We now describe two specific issues in more detail: the temporal drift in NOAA-15 channel 6, and the temporal drifts in channels 6–8 from NOAA-16.

3.3.1 NOAA-15 Channel 6

The results for NOAA-15 channel 6 are shown in Figure 7. Shortly after launch in May 1998 the drift for channel 6 is estimated at 19±4 MHz (one sample standard deviation), taken over the months August 1998 - February 1999. During this period the observed brightness temperatures are cold relative to the model background values resulting in a negative bias of -0.57±0.04 K during the same period. This negative bias relative to the ERA-Interim model increases steadily over the entire NOAA-15 data record, reaching -1.52±0.11 K in 2011. The standard deviation of the departures increases steadily during the period, from 0.25±0.01 K in 1998 to 0.37±0.04 K in 2011. There is also a pronounced seasonal cycle in the departure standard deviations. The derived pass band shift increases steadily, reaching a value of 44±6 MHz during 2011. This represents a frequency drift of 1.9 MHz.yr^{-1} during the period January 1999 - December 2011. The standard deviation of the departures computed using the new estimate of the center frequency is significantly lowered and is in line with the departures obtained from other sensors. Noteably, the seasonal cycle is eliminated. Also noteworthy is the change in the mean first guess departure which is close to zero, at -0.16±0.14K (1σ, standard deviation).

The shift in the NOAA-15 channel 6 pass band has been analysed independently by Zou and Wang (2011) who used simultaneous nadir overpasses of different satellites to diagnose a range of errors, including pass band shifts, in AMSU-A observations. The drift derived by Zou and Wang (2011), based on an analysis of data from July 2005 to September 2009, is 36.25±1.25 MHz. This value is in reasonable

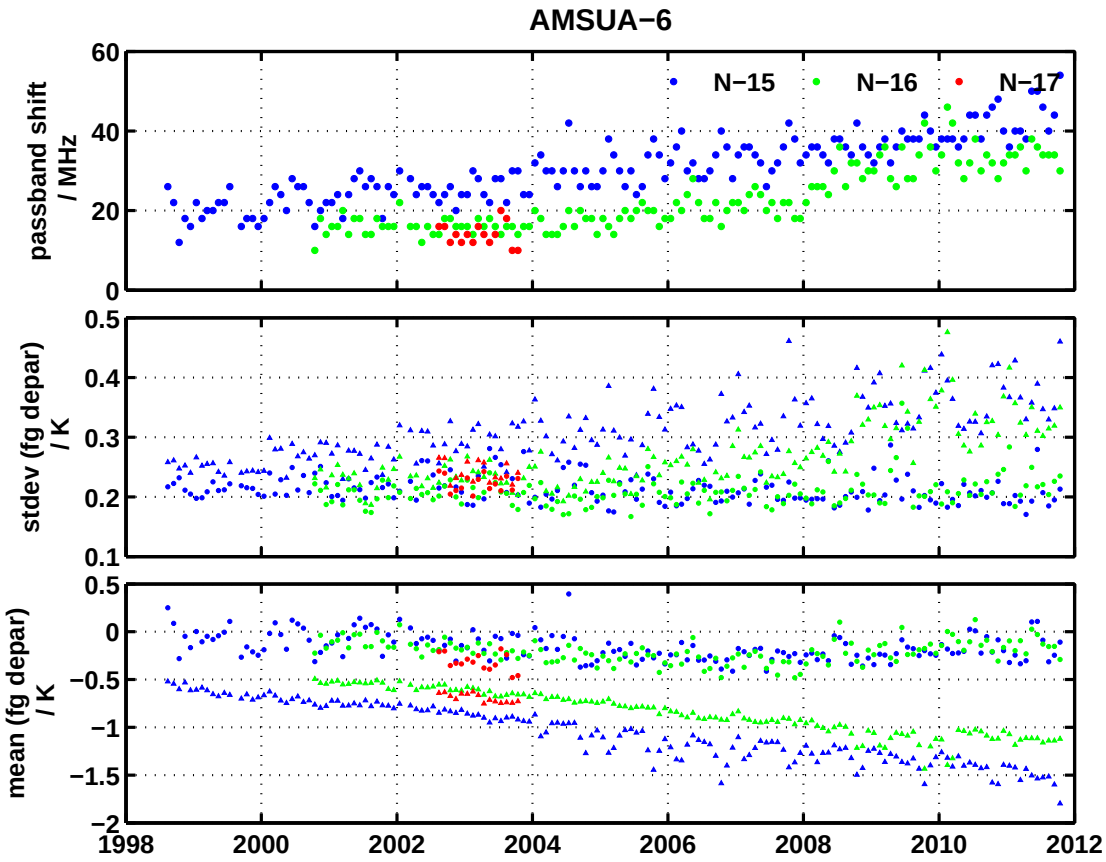

Figure 7: The evolution of channel center frequency shift estimates and associated departure statistics for AMSU channel 6 (nominally centered at 54.40 GHz) covering the period 1998-2012. Estimates were obtained from a single cycle each month during the period, on 15th of each month. The top plot shows the derived frequency drift. The middle shows the standard deviation of the first guess departures for unshifted (triangles) and shifted (circles) pass bands. The bottom plots shows the mean first guess departure for unshifted (triangles) and shifted (circles) pass bands. Results are shown for NOAA-15, -16, and -17.

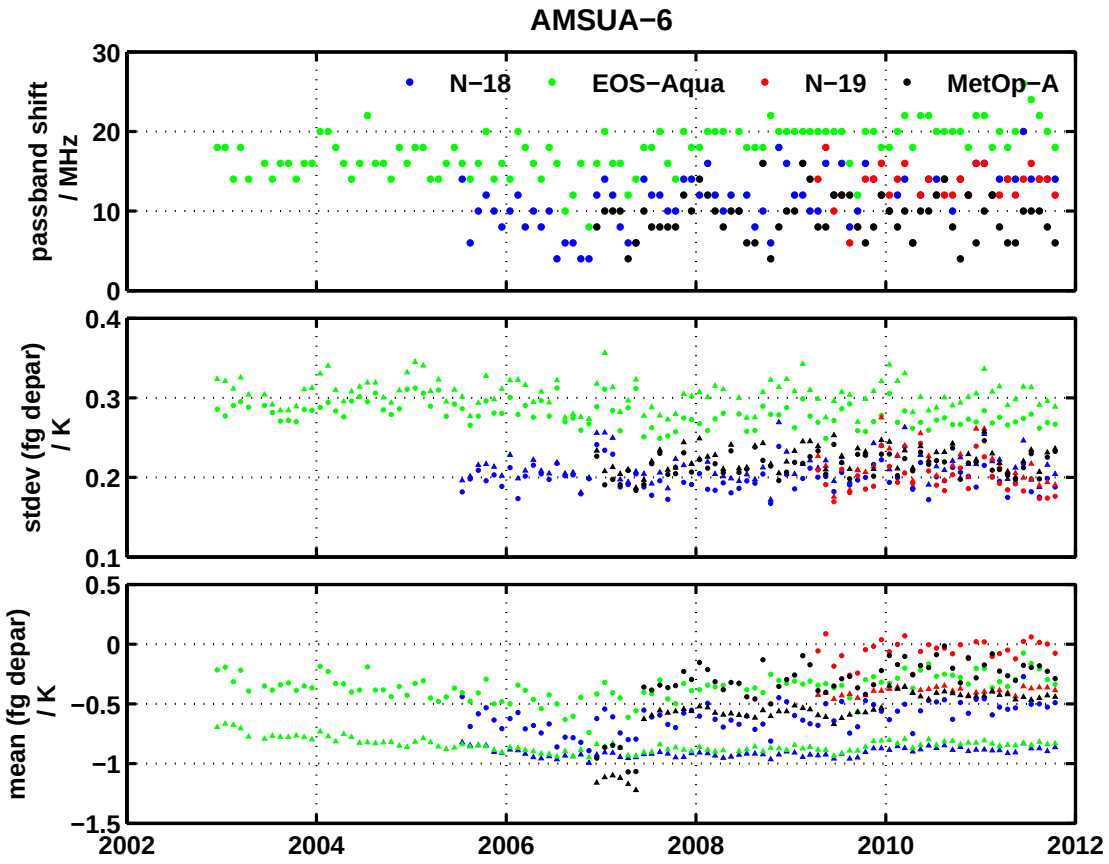

Figure 8: As for Figure 7. Results are shown for NOAA-18, -19, MetOp-A and NASA's EOS-Aqua.

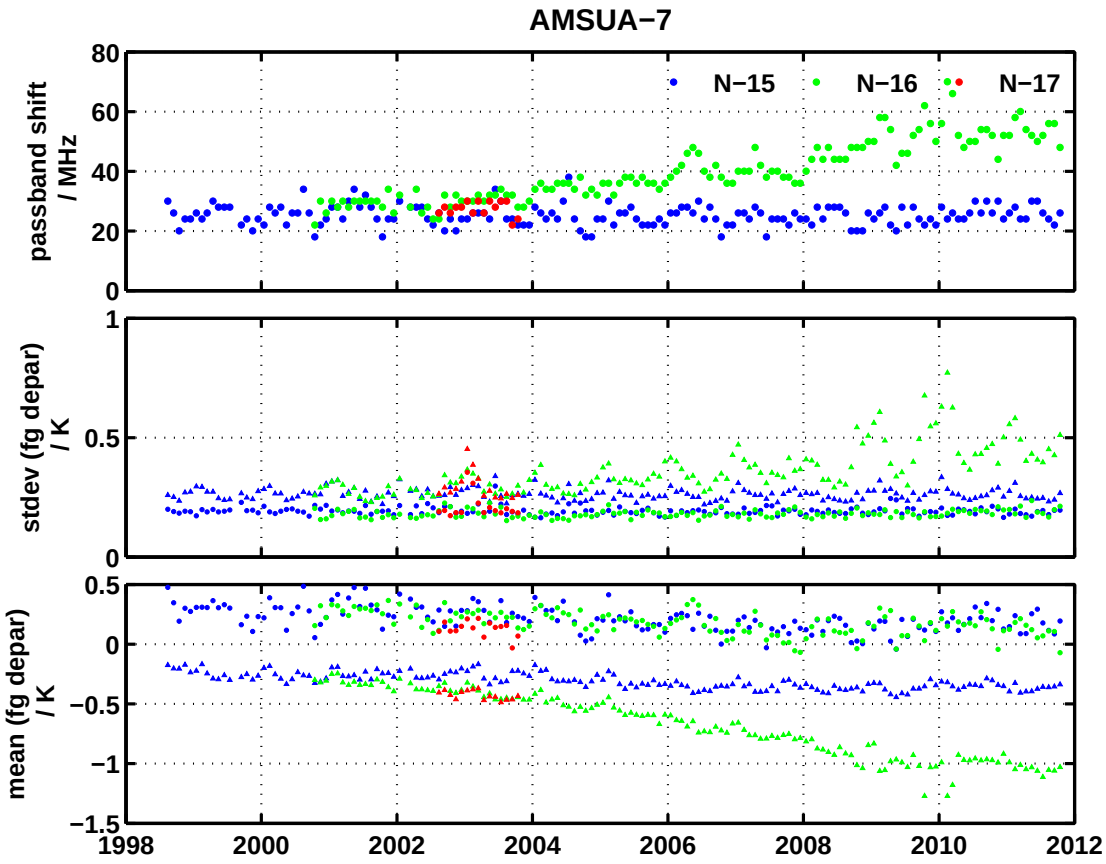

Figure 9: As for Figure 7, for AMSU channel 7 (nominally centred at 54.94 GHz)

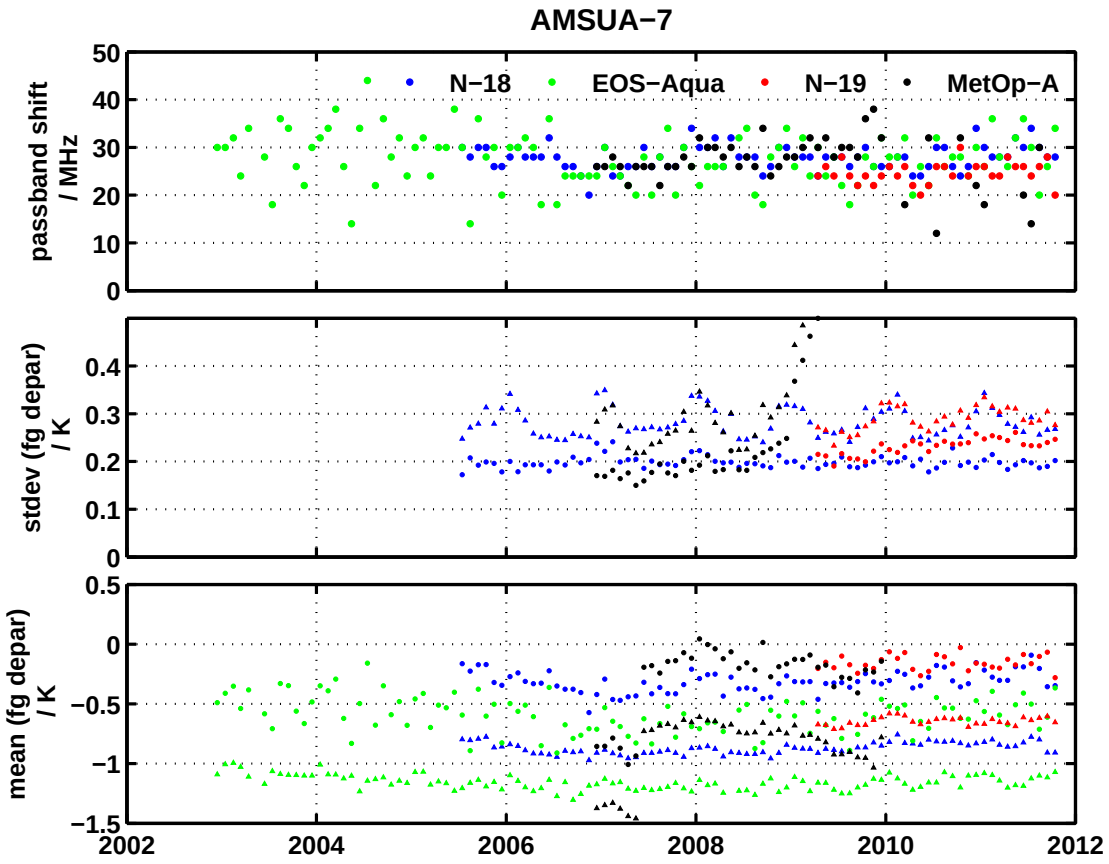

Figure 10: As for Figure 9. Results are shown for NOAA-18, -19, MetOp-A and NASA's EOS-Aqua.

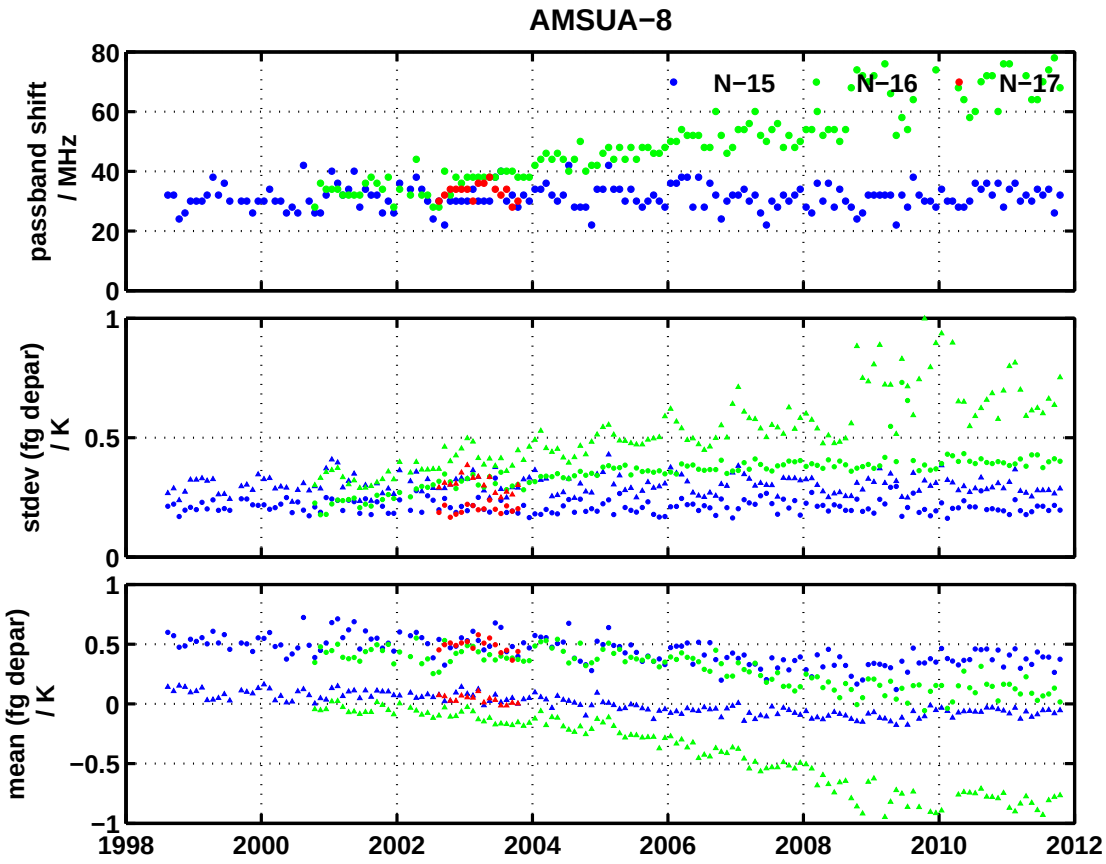

Figure 11: As for Figure 7, for AMSU channel 8 (nominally centered at 55.50 GHz)

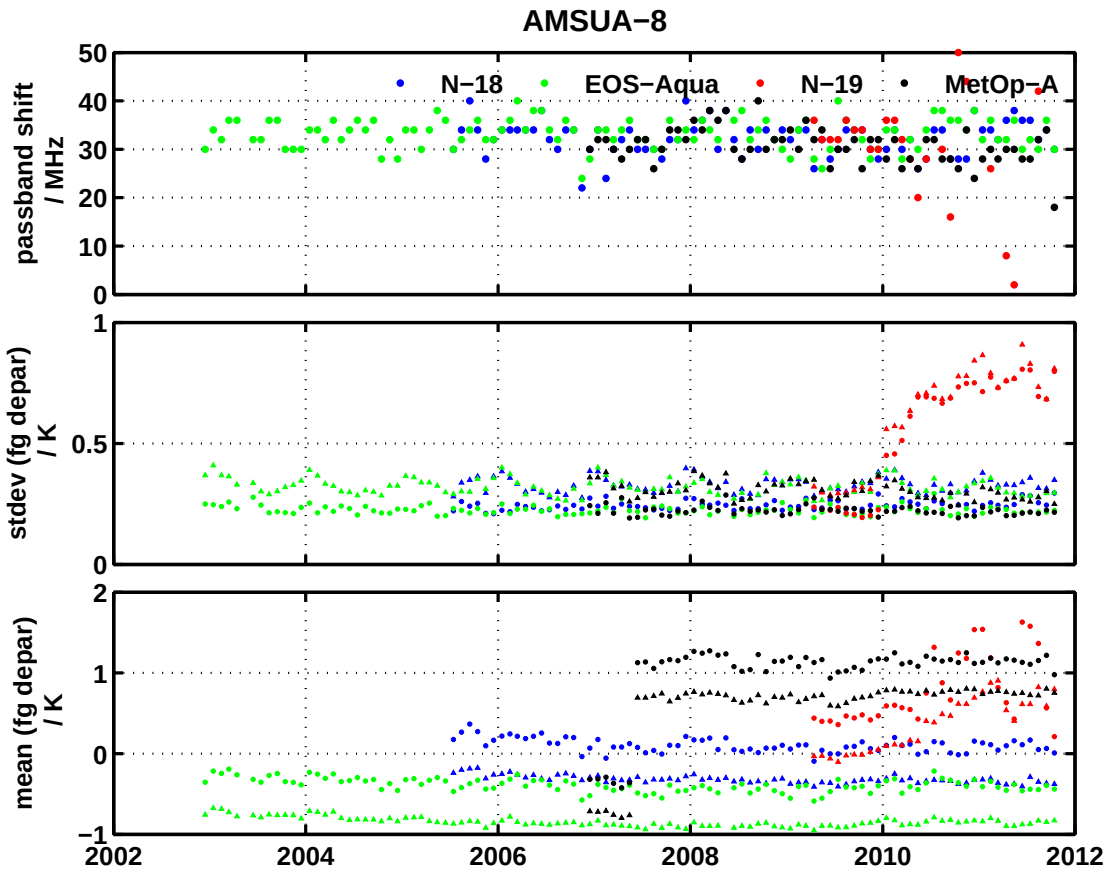

Figure 12: As for Figure 11. Results are shown for NOAA-18, -19, MetOp-A and NASA's EOS-Aqua.

agreement with the value derived here of 34±11 MHz (95% confidence interval) for the same period. Dee and Uppala (2009) have also commented on the drifts evident in this channel, based on the corrections derived through variational bias correction. As a result of the drift in bias and the large seasonal cycle in the departure statistics this channel has been blacklisted from the ECMWF operational system since February 2005. The improvement in data quality achieved by assuming the optimised center frequency suggests that pass band shift is the dominant problem for this channel and that the data could be rendered useful in data assimilation systems by computing new fast radiative transfer model coefficients at regular intervals.

3.3.2 NOAA-16 Channels 6-8

The results for NOAA-16 channels 6, 7 and 8 are shown in Figures 7, 9 and 11 respectively.

For channel 6, after launch in September 2000, the analysed shift appears stable at 16±3 MHz during the nine months of the satellite mission from October 2000 to June 2001. The shift remains stable until late 2005 when it begins to increase steadily, reaching 34±2 MHz during 2011. The mean departures decrease from -0.54±0.03 K during 2001 to -1.13±0.03 K during 2011. In addition the standard deviation of the departures is significantly larger than those for data using the improved pass band estimates and increases steadily after 2006 to values 50% larger, on average, than that for the new departures throughout 2011. The mean departures are improved from -0.85±0.23 K for data using the nominal pass bands, over the whole period, to -0.21±0.11 K for the data coumputed with the new pass band estimates.

For channel 7, the analysed shift appears stable at 28±3 MHz during the nine months following launch, remained stable until 2004, then increased to a value of 54±4 MHz by 2011. The mean departures decrease from -0.30±0.04 K during the first 9 months to -1.04±0.03 K during 2011. The standard deviation of the departures show a strong seasonal cycle with absolute values significantly higher than those for the data based on new estimates of the pass band throughout the entire period. The new data show reduced mean departures (0.18±0.10 K) over the whole period.

Channel 8 shows similar behaviour to channels 6 and 7. An initial shift of 33±2 MHz over the first nine months grows to 73±6 MHz during 2011. The seasonal cycle in the standard deviation of the original departures is eliminated and most of the trend in the mean departures is reduced through use of the new pass bands. It is clear, however, that the standard deviation of the corrected departures for Channel 8 show a significant increase over the period 2001-2011 suggesting that there is a more general deterioration in this particular channel.

3.4 Uncertainties

A complete and rigorous uncertainty analysis of the shift estimates presented here is beyond the scope of this paper. Such an analysis would take account of, among other factors, the uncertainties in the NWP model fields as well as the spectroscopic measurements underpinning the radiative transfer calculations. The analysis presented here yields sensible and conservative error bounds and takes account of the statistical component of the uncertainty (Type A errors as defined in BIPM (1998)) as well as the principal systematic components (more correctly termed Type B components BIPM (1998)).

The statistical components are straightforward to quantify and are derived from the reproducibility of the shift estimates over the stable periods in Figures 7 – 12. For most satellites and channels the stable period is the lifetime of the instrument, the exceptions being: NOAA-15 channel 6 (stable period June 1998–December 2000); NOAA-16 channels 6-8 (January 2001–November 2002); NOAA-18 channel 6

(October 2008 - October 2010) and NOAA-19 channel 8 (April 2009 - December 2009). The standard deviations of the shifts are given in Table 3 and for channels 6-8 are in the range ± 2 to ± 4 MHz. Normally the standard uncertainty on the mean shift would be obtained by dividing the standard deviation by $\sqrt{N}$, where N is the number of samples (here, assimilation cycles) from which the mean is derived. In this case, however, the values of $\Delta\nu$ reported in Table 3 are obtained from a single assimilation cycle and hence $N = 1$. The resulting standard error associated with statistical reproducibility, u_{STAT}, is taken to be equal to the standard deviation. The uncertainty components are summarised in Table 5.

The two sources of systematic error considered here are due to errors in the NWP model and errors in the underpinning spectroscopy, both of which could potentially project onto errors in the derived shifts.

The uncertainty component associated with the NWP model is derived from the range of shift values obtained from the four NWP models, as shown in Figure 5 and summarised in Table 4. It is assumed that the maximum deviation from the shift derived from the ECMWF based analysis represents the maximum range of a triangular distribution, $a_N = \pm|\Delta\nu_{ECMWF} - \Delta\nu_i|_{MAX}$. The standard deviation of this distribution ($u_{NWP} = a_N/\sqrt{6}$) gives the standard uncertainty associated with the NWP model. These uncertainty estimates vary between satellites and channels, but are typically in the range ± 3 to ± 9 MHz for channels 6-8 on most satellites.

The uncertainty associated with the underlying spectroscopy were estimated from the difference between the shifts derived from Liebe et al. (1992) and Tretyakov et al. (2005) (a_{RT}) as shown in Table 3. In this case a rectangular distribution was assumed, with standard deviation $u_{RT} = a_{RT}/\sqrt{3}$. These are $\pm$6MHz in the largest case, for channels with significant diagnosed shifts. Uncertainties associated with the numerical integration of the radiative transfer model are assumed to be small in comparison.

Following BIPM (1998) these components are combined to produce a combined standard uncertainty, u_{TOT}:

$$u_{TOT}^2 = u_{STAT}^2 + u_{NWP}^2 + u_{RT}^2 \tag{1}$$

And finally a 95% confidence interval, $U(\Delta\nu)$, is derived:

$$U(\Delta\nu) = k u_{tot} \tag{2}$$

In this case assuming a coverage factor of $k = 2$. The final expanded uncertainties are in the range $\pm$ 10 - 14 MHz for most channels. It's noteworthy that these derived uncertainty estimates, if interpreted as detection sensitivities, are in approximate agreement with the intuitively derived criteria: that shifts that are ascribed significance should be associated with reductions in the standard deviations of first guess departures of 10% or more. For example, for channel 6 on NOAA-18,-19, MetOp-A and Aqua the derived shifts are in the range 10-18 MHz (Table 3), close to the 95% confidence intervals derived here, but do not lead to reductions in standard deviations in departures of more than 10%.

4 Frequency drift analysis for MSU Channel 3

4.1 Time series of MSU Channel 3 Drifts

Pass band shifts were analysed for MSU channel 3 (54.96 GHz) for the years 1979 to 2007. This analysis includes data from TIROS-N and the NOAA satellites NOAA-6 to -10, -12 and -14. The NOAA-13 satellite only operated for 12 days due to a power failure. Channels 1 (50.3 GHz) and 2 (52.8 GHz) are affected by clouds (with cloud signals as large as 10K and 2K respectively) which complicated the analysis presented here: deficiencies in any cloud detection algorithm could potentially result in errors in model cloud fields being aliased into the analysis of pass band centers. An analysis of the pass band center for channel 4 was found to be flawed due to an erroneous assumption about the form of the band and will be a topic of further study. Figure 13 shows the derived shifts for Channel 3. The results are summarised in Table 6.

Large shifts are evident for the early MSU instruments, on satellites from TIROS-N to NOAA-10. The largest shift occurs for TIROS-N at 68 ± 4 MHz for the period January 1979 - February 1981. Most shifts appear to remain constant from the earliest post-launch period through the lifetime of the satellites, with the exception of NOAA-6 which shows an initial shift of 40 MHz rising to 60 MHz from mid 1979 to 1981. Thereafter the shift is stable at 60 MHz until the end of the mission in 1987, although there is a significant outage from 1984 to mid-1985. The large seasonal variability of $\sim$ 30% in the standard deviation of the departures for the MSUs on TIROS-N, NOAA-6, -7, -8, -9 and -10 is effectively eliminated through use of the corrected center frequencies, lending weight to the argument proposed here that the variance in the observation-simulated differences is dominated by the biases due to the shift. Another aspect of this analysis lends weight to this argument; the mean departures are improved significantly for most MSUs through use of the modified center frequencies, the single exception here is NOAA-12 where the mean departure increases from 0 to 0.3K. For all other MSUs the mean departure is shifted towards zero. For NOAA-6, for example, a bias of 1-2K obtained for the nominal frequency is reduced to less than 0.5K through use of the improved estimate. This result is noteworthy - the metric used to optimise the pass band center frequency estimate is the variance of the departures, any improvement in the mean departure is a by product of the analysis, and yet the improved center frequency estimates result in generally improved biases, with the exception of NOAA-12. For NOAA-10 the mean departure is improved, from $\sim$ -2.2K to -1.2K, but remains large.

Overall these results indicate the radiometric accuracy of the MSUs is much better that previously thought. When the spectral shifts are taken into account correctly in the forward model of the radiances then the biases between observations and model are reduced to 0.5K or better. This suggests the radiometric calibration of the MSUs, for this channel, are consistent between satellites to 0.5K.

5 Conclusion and Discussion

This study has analysed shifts in the pass band center frequencies for a number of microwave sounding instruments on past and present meteorological satellites. Large shifts, relative to nominal center frequencies, have been determined for key tropospheric sounding channels of AMSU-A and MSU for most satellites. No significant drift has been determined for AMSU-A channels 9-14. Including these refined estimates of the channel center frequencies in fast radiative transfer models results in improved fit between observations and model, reduced seasonal variability in the observation-model misfit and significantly improved biases between model and observations. For some channels on some satellites there is evidence of significant drifts with time (for example NOAA-15 channel 6 and NOAA-16 channels 6, 7 and 8). However, for most channels studied the shifts take the form of a constant offset throughout the life of the satellite. Newly available spectroscopic parameters, derived from improved measurements of the O_2 absorption complex, have been tested. Although there is evidence that the new spectroscopy results in better model-observation fit for channel 10, the results from the new spectroscopy for the lower peak-

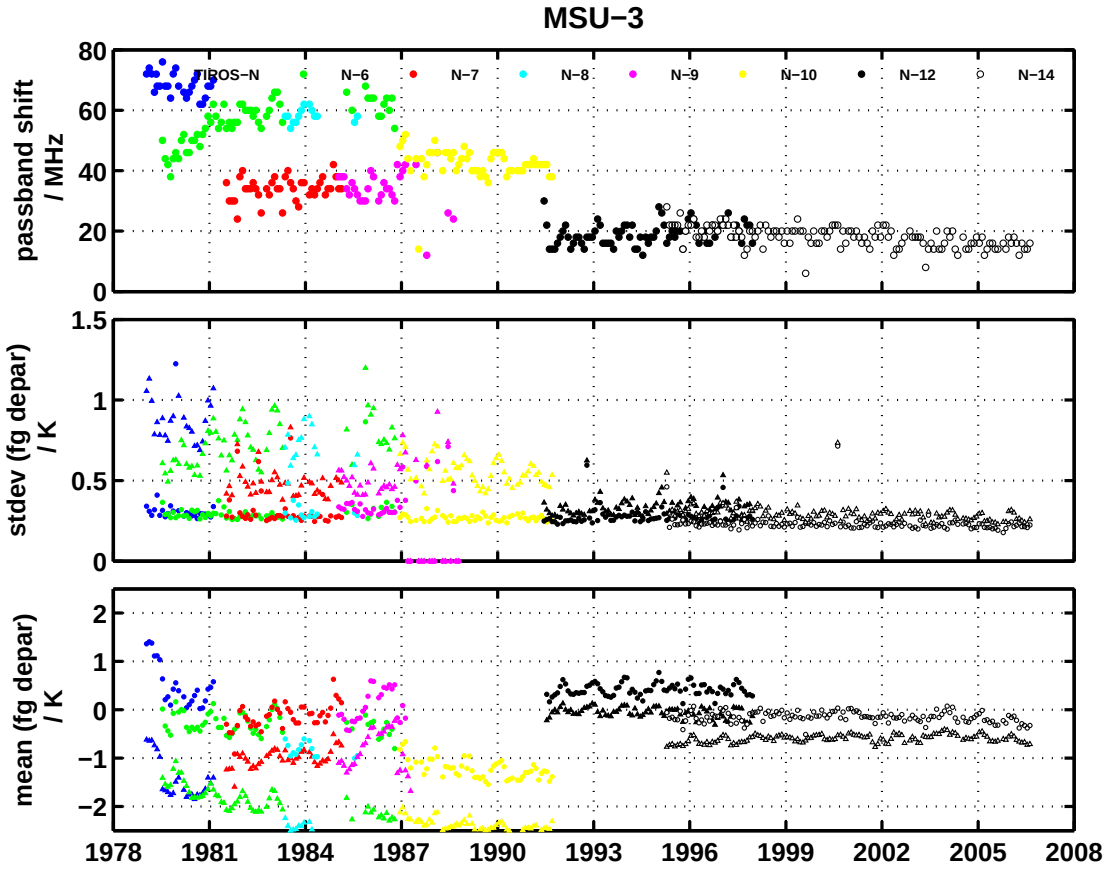

Figure 13: The evolution of channel center frequency shift estimates and associated departure statistics for MSU channel 3 (nominally centered at 54.74 GHz) covering the period 1978-2007. Estimates were obtained from a single cycle each month during the period, on 15th of each month. The top plot shows the derived frequency drift. The middle shows the standard deviation of the first guess departures for unshifted (triangles) and shifted (circles) pass bands. The bottom plots shows the mean first guess departure for unshifted (triangles) and shifted (circles) pass bands. Results are shown for TIROS-N, NOAA-6, -7, -8, -9, -10, -12 and -14.

ing channels (AMSU-A 6-8) are broadly in agreement with the results from the MPM92 spectroscopy and do not change the main conclusions reported here. Previous independent studies have determined a significant center frequency shift for AMSU chanel 6 on NOAA-15 and the results reported here are in good agreement with this independent determination.

The stark contrast between the significant shifts detected for channels 6-8 and the lack of any significant shifts determined for channels 9-14 supports the hypothesis that the shifts are real and due to the uncertainties, shifts and drifts in the passively stabilised local oscillators which serve all channels up to channel 8, channels 9-14 being served by a single actively locked local oscillator.

The bias introduced by these center frequency uncertainties is complex and state-dependent. The bias depends on the local temperature lapse rate in the region around the displaced weighting function peak. For example, Lu et al. (2011a) showed that a pass band shift affecting a channel with a weighting function peak in the lower stratosphere (the FY-3A Microwave Temperature Sounder channel 4 at 57.29 GHz) will result in a strong positive brightness temperature bias in the tropics where there is a strong positive lapse rate. In the high latitudes where the lapse rate is much smaller, the resulting bias is smaller. The main signature of such a bias is an apparent airmass dependent bias but also a weaker cross-scan bias as identified by Peubey et al. (2011). Within NWP systems these biases have been corrected using air mass predictors as well as γ-corrections.

One conclusion from this study is that the correction of these errors results in much improved biases with respect to NWP models. Agreement is generally 0.5K or better for AMSU-A channels 6-8 for most satellites, prior to bias correction. This suggests that a major contribution to the observed observation-model offsets and the observed inter-satellite offsets, often attributed to *radiometric* calibration uncertainties, is actually the differing *spectral* characteristics of the instruments. That is to say, the radiometric accuracies of these microwave instruments is better than previously thought, and is around $\pm$ 0.5K. This means that, with some improvements in pre-launch spectral and radiometric characterisation and the adoption of active phase-locking for temperature sounding channels, future microwave radiometers may be able to meet the exacting requirements for climate quality data.

This study raises several questions: firstly, given the large amplitude of the shifts, why have these not been identified in previous studies ? With the exception of the study of Zou and Wang (2011) which detected a 36 MHz shift for AMSU channel 6 on NOAA-15, no other previous analyses have reported such large shifts. The largest effects reported here are for NOAA-16 channels 6, 7 and 8. Zou and Wang (2011) and Mears and Wentz (2009) comment on the radiometric drift in NOAA-16 channels 5, 7 and 9 (and other, unspecified, channels) and consequently exclude these channels from their climate analyses. The remaining AMSU-A channel 7 and 8 pass band shifts are relatively stable and similar in magnitude (26-38 MHz) for the other satellites. The similarity of the diagnosed shift for these satellites for these channels means that any analysis method based on inter-satellite differences would be relatively insensitive to the absolute value of the shift. It is possible that the range of differences (12 MHz) is close to the effective detection sensitivity for the SNO techniques used in the study of the NOAA-15 channel 6 drift.

Is it possible that the shifts are actually much closer to zero and some other spectroscopic or forecast model error is being aliased into the shift estimate ? The counter-arguments here are the elimination of the strong seasonal cycles, evident for NOAA-18,-19, MetOp-A and Aqua during functioning periods, as well as the sharp discontinuity in derived shifts for channels 6–8 versus channels 9 and above. The simplest explanation of these results is that the shifts are real and affect, to some degree, most of the passively stabilised channels studied.

We expect significant benefits for the exploitation of this microwave data in atmospheric reanalysis as a result of these results. The use of improved observation operators (through improved radiative transfer

modelling) is expected to lead to significant reductions in the corrections necessarily applied to this data, and to reductions in the amplitude of residual local biases remaining after bias correction, as a result of a more accurate treatment of the biases through improved understanding of the underlying mechanisms. Work is ongoing to assess the new radiative transfer modelling in atmospheric reanalyses: the new modelling will be incorporated in the next generation ECMWF reanalysis system, due to commence in January 2014.

In the longer term we hope this study will lead to a refinement of the specification and design of microwave sounding instruments for future operational missions, to improve the stability of local oscillators and to continue to improve the pre-launch characterisation, both spectral and radiometric. Given the unexpectedly good radiometric performance of the AMSU-A instruments, we hope this study will invigorate research and development work aimed at improving the absolute radiometric accuracy of microwave sounders on-orbit, in the hope that future sensors will meet the needs of climate and NWP, reducing the role of complex *ad-hoc* correction methods.

Finally, we hope to extend the work to cover the channels more commonly used for climate studies (AMSU-A channel 5 and MSU channels 2 and 4).

Acknowledgments

This work was supported by EUMETSAT's NWP-SAF Visiting Scientist Programme which supported the visit of Dr Qifeng Lu to ECMWF during 2011-12. The work was also supported by China's Research and Development Special Fund for Public Welfare Industry [GYHY201206002] and the National Natural Science Foundation of China (Grant No. 40705037). The authors thank Tony McNally (ECMWF) for arranging this visit, and Niels Bormann, Carole Peubey and Steve English (ECMWF) for helpful discussions on the work. Michail Tretyakov is thanked for providing the new spectroscopic parameters and for advice. Richard Renshaw at the Met Office kindly provided Met Office analysis fields for the study. Paul Poli (ECMWF), John Eyre (Met Office), Jean-Noël Thépaut (ECMWF) and Christophe Accadia (EUMETSAT) are thanked for their careful reviews of the manuscript and constructive comments which have improved it significantly.

References

Auligné, T., A. P. McNally, and D. P. Dee (2007). Adaptive Bias Correction for Satellite Data in a Numerical Weather Prediction System. *Q. J. R. Met. Soc. 133*, 631–642.

Bell, W., S. J. English, B. Candy, N. Atkinson, F. Hilton, N. Baker, S. D. Swadley, W. F. Campbell, N. Bormann, G. Kelly, and M. Kazumori (2008). The Assimilation of SSMIS Radiances in Numerical Weather Prediction Models. *IEEE Transactions on Geoscience and Remote Sensing 46*, 884–900.

BIPM (1998). Evaluation of measurement data - Guide to the expression of uncertainty in measurement.

Cardinali, C. (2009). Monitoring the observation impact on the short-range forecasts. *Q. J. R. Met. Soc. 135*, 239–250.

Christy, J., R. W. Spenser, and E. S. Lobel (1998). Analysis of the merging procedure for the MSU daily temperature time series. *J. Climate 11*, 2016–2041.

Collard, A. D. and A. P. McNally (2009). The assimilation of Infrared Atmospheric Sounding Interferometer radiances at ECMWF. *Q. J. R. Met. Soc. 135*, 1044–1058.

Courtier, P., J.-N. Thépaut, and A. Hollingsworth (1994). A strategy for operational implementation of 4D-Var, using an incremental approach. *Q. J. R. Met. Soc. 120*, 1367–1387.

Dee, D. P. and S. Uppala (2009). Variational bias correction of satellite radiance data in the ERA-Interim reanalysis. *Q. J. R. Met. Soc. 135*, 1830–1841.

Dee, D. P., S. M. Uppala, A. J. Simmons, P. Berrisford, P. Poli, S. Kobayashi, U. Andrae, M. A. Balmaseda, G. Balsamo, P. Bauer, P. Bechtold, A. C. M. Beljaars, L. van de Berg, J. Bidlot, N. Bormann, C. Delsol, R. Dragani, M. Fuentes, A. J. Geer, L. Haimberger, S. B. Healy, H. Hersbach, E. V. Hlm, L. Isaksen, P. Kllberg, M. Khler, M. Matricardi, A. P. McNally, B. M. Monge-Sanz, J.-J. Morcrette, B.-K. Park, C. Peubey, P. de Rosnay, C. Tavolato, J.-N. Thépaut, and F. Vitart (2011). The ERA-Interim reanalysis: configuration and performance of the data assimilation system. *Q. J. R. Met. Soc. 137*, 553–597.

Dong, C., J. Yang, W. Zhang, Z. Yang, N. Lu, J. Shi, P. Zhang, Y. Liu, and B. Cai (2009). An Overview of Chinese New Weather Satellite FY-3A. *Bulletin of The American Meteorological Society 90*, 1531–1544.

Goodrum, G., K. B. Kidwell, and W. Winston (2000). NOAA KLM Users Guide.

Harris, B. A. and G. Kelly (2001). A satellite radiance bias correction scheme for data assimilation. *Q. J. R. Met. Soc. 127*, 1453–1468.

Healy, S. and J.-N. Thépaut (2006). Assimilation experiments with CHAMP GPS radio occultation measurements. *Q. J. R. Met. Soc. 132*, 605–623.

Iacovazzi, R. A., C. Cao, and S.-A. Boukabara (2009). Analysis of polar-orbiting operational environmental satellite NOAA-14 MSU and NOAA-15 AMSU microwave sounders for climate change detection. *Journal of Geophysical Research 114*.

JPL (2000). AIRS Project Algorithm Theoretical Basis Document, Level 1b, Part 3: Microwave Instruments.

Liebe, H. J., Rosenkranz, P.W., and G. Hufford (1992). Atmospheric 60-GHz Oxygen Spectrum: New Laboratory Measurements and Line Parameters. *Journal of Quantitative Spectroscopy and Radiative Transfer 48*, 629–643.

Lu, Q., W. Bell, P. Bauer, N. Bormann, and C. Peubey (2011a). Characterizing the FY-3A microwave temperature sounder using the ECMWF model. *J.Atmospheric and Oceanic Technology 28*.

Lu, Q., W. Bell, P. Bauer, N. Bormann, and C. Peubey (2011b). Improved assimilation of data from china's FY-3A microwave temperature sounder. *Atmospheric Science Letters 13*.

McNally, A. P., J. C. Derber, W. Wu, and B. B. Katz (2000). The use of TOVS level-1b radiances in the NCEP SSI analysis system. *Q. J. R. Met. Soc. 126*, 689–724.

Mears, C. and F. J. Wentz (2009). Construction of the Remote Sensing Systems V3.2 atmospheric temperature records from the MSU and AMSU microwave sounders. *J. Atmos. Oceanic Techn. 26*, 3650–3664.

Mo, T., M. D. Goldberg, D. S. Crosby, and Z. Cheng (2001). Recalibration of the NOAA Microwave Sounding Unit. *Journal of Geophysical Research 106*, 10,145–10,150.

Peubey, C., W. Bell, P. Bauer, and S. D. Michele (2011). A Study on the Spectral and Radiometric Specifications of a post-EPS Microwave Imaging Mission. In *ECMWF Technical Memorandum Number 643*, ECMWF, Shinfield Park, Reading, UK. ECMWF.

Rawlins, F., S. P. Ballard, K. J. Bovis, A. M. Clayton, D. Li, G. W. Inverarity, A.C.Lorenc, and T. J. Payne (2007). The Met Office Global Four Dimensional Variational Assimilation Scheme. *Q. J. R. Met. Soc. 133*, 347–362.

Smith, W. L., H. Woolf, C. M. Hayden, A. J. Schreiner, and J. F. LeMarshall (1983). The Physical Retrieval TOVS Export Package.

Tretyakov, M. Y., M. A. Koshelev, and V. V. Dorovskikh (2005). 60-GHz oxygen band: precise of fine-structure lines, broadening and central frequencies absolute absorption profile at atmospheric pressure, and revision of mixing coefficients. *Journal of Molecular Spectroscopy 231*, 1–14.

Zou, C.-Z. and W. Wang (2011). Intersatellite calibration of AMSU-A observations for weather and climate applications. *Journal of Geophysical Research 116*(D23113).

Table 1: AMSU-A channel characteristics

Channel no.	Frequency / GHz	Bandwidth / MHz	Stability / MHz (design spec)
6	54.40	400	$\pm$5
7	54.94	400	$\pm$5
8	55.50	330	$\pm$10
9	f_0=57.290344	330	$\pm$0.5
10	$f_0\pm$0.217	78	$\pm$0.5
11	$f_0\pm$0.322.2$\pm$0.048	36	$\pm$1.2
12	$f_0\pm$0.322.2$\pm$22	16	$\pm$1.2
13	$f_0\pm$0.322.2$\pm$10	8	$\pm$0.5
14	$f_0\pm$0.322.2$\pm$4.5	3	$\pm$0.5

Table 2: NWP model characteristics

NWP Center / model	Model characteristics
ECMWF IFS	T511 L91
Met Office UM	N520 L70
NCEP	T574 L64
CMA	T636 L60
ECMWF ERA-Interim	T255 L90

Table 3: Optimised pass band center frequency shifts for AMSU-A channels 6-14. Shifts are expressed relative to nominal pass band centers in Table 1. **Bold** underlined entries indicate significant shifts, where the reduction in the standard deviation of the departures exceeds 10%. Italicised entries indicate where a channel is known to suffer from problems other than pass band shifts. Estimates are shown for both Liebe et al. (1992) (**MPM92**) and Tretyakov et al. (2005) (**TR05**) models. The $\pm 1\sigma_{\Delta\nu}$ standard deviations represent the reproducibility of the estimates computed for the stable periods of the time series data shown in Figures 7 - 12, for the **MPM92** spectroscopy.

Channel		$\Delta\nu \pm 1\sigma_{\Delta\nu}$ / GHz (% reduction in STDEV (departures))					
		NOAA-15	NOAA-16	NOAA-18	NOAA-19	MetOp-A	EOS-Aqua
6	MPM92	**40±4 (40.2)**	**26±2 (20.6)**	14±3 (9.5)	12±3 (4.6)	10±3 (2.3)	18±3 (6.9)
	TR05	**38 (38.3)**	**26 (18.4)**	12 (7.1)	10 (3.0)	8 (1.1)	16 (5.5)
7		**24±3 (17.6)**	**52±3 (50.2)**	**30±3 (28.0)**	**26±2(14.9)**	*36±3 (0.6)*	*26±6 (1.1)*
		20 (13.1)	**48 (47.9)**	**28 (23.6)**	**24 (11.5)**	*36 (0.6)*	*26 (0.8)*
8		**28±4 (13.8)**	**68±4 (32.0)**	**36±4 (21.4)**	*32±2 (2.8)*	**32±4 (18.7)**	**38±3 (34.6)**
		22 (9.2)	**66 (29.9)**	**32 (16.6)**	*26 (1.8)*	**28 (14.1)**	**34±3 (28.7)**
9		30 (3.5)	0 (0.0)	12 (0.3)	16 (0.7)	0 (0.0)	20 (1.8)
		22 (1.5)	0 (0.0)	0 (0.0)	2 (0.0)	0 (0.0)	12 (0.3)
10		14 (4.0)	0 (0.0)	16 (6.2)	18 (7.2)	12 (2.6)	14 (4.9)
		10 (1.1)	0 (0.0)	12 (2.6)	14 (3.4)	6 (0.2)	10 (1.5)
11		*25 (6.3)*	0 (0.0)	7 (0.8)	7 (1.0)	4 (0.0)	11 (4.6)
		25 (6.3)	0 (0.0)	5 (0.3)	6 (0.5)	0 (0.0)	10 (3.1)
12		3 (0.8)	0 (0.0)	3 (0.6)	3 (0.4)	5 (2.1)	2 (0.1)
		12 (0.2)	0 (0.0)	3 (0.3)	6 (0.5)	0 (0.0)	10 (3.1)
13		1 (0.2)	**5 (13.2)**	0 (0.0)	0 (0.0)	3 (5.0)	0 (0.0)
		1 (0.0)	**5 (12.2)**	0 (0.0)	0 (0.0)	3 (4.4)	0 (0.0)
14		**5 (47.9)**	**2 (18.0)**	0 (0.0)	1 (0.4)	2 (2.8)	1 (0.5)
		5 (48.0)	**2 (17.3)**	0 (0.0)	1 (0.3)	2 (2.7)	1 (0.3)

Table 4: Derived shifts for four different NWP models

Channel number		Δν / GHz N-15	N-16	N-18	N-19	MetOp-A	Aqua
6	ECMWF	40	26	15	12	10	18
	Met Office	50	38	26	24	22	30
	NCEP	38	26	12	12	10	20
	CMA	42	32	18	18	8	22
$a_N = \pm\lvert\Delta\nu_{ECMWF} - \Delta\nu_i\rvert_{MAX}$		±**10**	±**12**	±11	±12	±12	±12
$u_{NWP} = a_N/\sqrt{6}$		±**4.1**	±**4.9**	±4.5	±4.9	±4.9	±4.9
7		24	52	30	26	36	18
		38	60	46	40	40	30
		24	52	44	26	80	20
		30	58	36	34	80	22
$a_N = \pm\lvert\Delta\nu_{ECMWF} - \Delta\nu_i\rvert_{MAX}$		±**12**	±**8**	±**16**	±**14**	±44	±12
$u_{NWP} = a_N/\sqrt{6}$		±**4.9**	±**3.3**	±6.5	±5.7	±18.0	±4.9
8		28	68	36	32	32	38
		50	72	58	54	48	58
		34	74	44	36	38	46
		44	78	52	50	46	54
$a_N = \pm\lvert\Delta\nu_{ECMWF} - \Delta\nu_i\rvert_{MAX}$		±**22**	±**4**	±**22**	±**22**	±16	±20
$u_{NWP} = a_N/\sqrt{6}$		±**9.0**	±**1.6**	±9.0	±9.0	±6.5	±8.2
9		30	0	12	16	0	20
		0	0	0	0	0	0
		18	0	0	0	0	4
		8	0	0	0	0	0
$a_N = \pm\lvert\Delta\nu_{ECMWF} - \Delta\nu_i\rvert_{MAX}$		±30	±0	±12	±16	±0	±12
$u_{NWP} = a_N/\sqrt{6}$		±12.2	±0.0	±4.9	±6.5	±0.0	±4.9
10		16	0	16	18	12	14
		0	0	0	0	0	0
		26	10	22	22	22	22
		30	14	28	24	26	26
$a_N = \pm\lvert\Delta\nu_{ECMWF} - \Delta\nu_i\rvert_{MAX}$		±14	±14	±12	±6	±14	±12
$u_{NWP} = a_N/\sqrt{6}$		±5.7	±5.7	±4.9	±2.4	±5.7	±4.9
11		25	0	7	7	4	11
		25	0	11	12	9	14
		25	1	1	1	1	1
		25	1	1	1	1	1
$a_N = \pm\lvert\Delta\nu_{ECMWF} - \Delta\nu_i\rvert_{MAX}$		±0	±1	±4	±6	±5	±10
$u_{NWP} = a_N/\sqrt{6}$		±0.0	±0.4	±1.6	±2.4	±2.0	±4.1

Table 5: Pass band Shifts for AMSU-A Channels 6-8 together with expanded uncertainty estimates.

Channel number		Δν, Component standard, and expanded, uncertainties in MHz N-15	N-16	N-18	N-19	MetOp-A	Aqua
6	$u_{STAT} = \sigma_{\Delta\nu}/\sqrt{N}$	4	2	3	3	3	3
	u_{NWP}	4	5	4	5	5	5
	u_{RT}	1	0	1	1	1	1
$\Delta\nu \pm U_{\Delta\nu}$		**40±11**	**26±11**	14±10	12±12	10±12	18±12
7	$u_{STAT} = \sigma_{\Delta\nu}/\sqrt{N}$	3	3	3	2	3	6
	u_{NWP}	5	3	6	6	18	5
	u_{RT}	4	4	2	2	0	24
$\Delta\nu \pm U_{\Delta\nu}$		**24±14**	**52±12**	**30±14**	**26±14**	*36±36*	*26±50*
8	$u_{STAT} = \sigma_{\Delta\nu}/\sqrt{N}$	4	4	4	2	4	3
	u_{NWP}	9	2	9	9	6	8
	u_{RT}	6	2	4	6	4	4
$\Delta\nu \pm U_{\Delta\nu}$		**28±23**	**68±10**	**36±21**	*32±22*	**32±16**	**38±19**

Table 6: Center frequency shifts for MSU channel 3. Channel shifts and related statistics are computed for the stable periods indicated.

Satellite	Stable Period	$\Delta\nu$ / MHz	Δstdev(fg dep) / %
TIROS-N	1/1979–2/1981	68.4$\pm$3.7	63.0$\pm$9.8
NOAA-6	2/1981–10/1986	59.9$\pm$3.9	59.9$\pm$8.8
NOAA-7	7/1981–2/1985	33.9$\pm$3.8	34.0$\pm$13.5
NOAA-8	5/1983–8/1985	58.1$\pm$2.3	56.8$\pm$9.2
NOAA-9	1/1985–2/1987	35.0$\pm$3.9	33.8$\pm$7.6
NOAA-10	10/1987–9/1991	42.5$\pm$3.2	50.3$\pm$7.6
NOAA-12	6/1991–12/1997	19.1$\pm$3.6	18.0$\pm$6.7
NOAA-14	4/1995–8/2006	18.1$\pm$3.4	20.7$\pm$7.2